Death near the Shoreline, not Life on Land: Ordovician Arthropod Trackways in the Borrowdale Volcanic Group, UK

Anthony P. Shillito and Neil S. Davies

STRATIGRAPHIC CONTEXT OF THE TRACKWAYS

The Lum Pot site, where the arthropod trackways occur, was described as being in the Dunnerdale Sandstone Formation (DNF) by Johnson et al. (1994), and is presently mapped as such by the British Geological Survey (BGS). In this paper we consider it more likely that the trackways are within the Wallowbarrow Tuff Formation (WAL), which is a localized stratigraphic unit bounded above and below by the DNF (Figure 1B). This conclusion is based on the fact that the lithology of the Lum Pot stream section consists of at least 14 meters of continuous tuff, whereas, by definition, the DNF consists entirely of volcanoclastic sandstones and breccia (Millward, 2004). The sandstone lithology of the trackway beds, as previously reported, was inconsistent and incorrect (described by Johnson et al. (1994) variably as fine-grained sandstone (p. 397, 404), fine- to medium-grained sandstone (p. 397) or medium- to coarse-grained sandstone (p. 398, 399)). Additionally, the presence of WAL at the locality is not surprising: whilst existing BGS bedrock maps show the predicted DNF/WAL boundary to be approximately 200 meters upstream on the River Lickle from Lum Pot, such a boundary is not exposed in the field. The drift cover, extensive faulting, and lack of continuous exposure in the area means that existing maps are, at least in part, conjectural but the re-identification of the Lum Pot rocks as tuff (as originally noted by Mitchell, 1956) identifies the WAL as the most likely host stratigraphic unit (Figure S1).

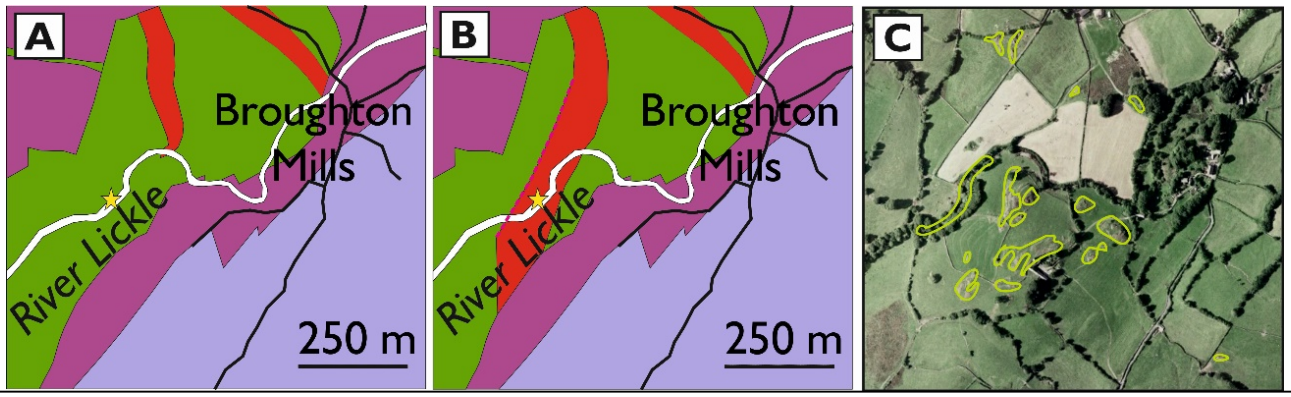

Figure S1. ***Geological maps of the Lum Pot site, with trace-fossil site starred. WAL shown in red and DNF in green: see Figure 1 for full key. A) Current BGS map; B) Proposed map, based on tuff outcrop along the River Lickle; C) Limited outcrop exposure (highlighted in green) on which map in A was based. © 2018 Google Earth, Infoterra & Bluesky.***

TRACKWAY SURFACES

Johnson et al. (1994) recorded two trackway-bearing surfaces at Lum Pot: a bed with abundant trails on top (here, Surface C1), and a bed with sparse trails on a rippled surface (here, Surface B). In this study we identified three further surfaces bearing trackways, referring to them in stratigraphic order from oldest to youngest (A, B, C1, C2, and D, where C2 is a different surface of the same bed as C1, exposed on the south side of the River Lickle). A description of each of the trackway bearing surfaces, and their position in the local stratigraphy, is shown in Table S1. The outcrop of each surface is shown in Figures S2-S6, with trackways traced onto the photographs in pink (*Diplopodichnus*) and blue (*Diplichnites*).

Figure S2. ***Surface A (ruler is 24 cm).***

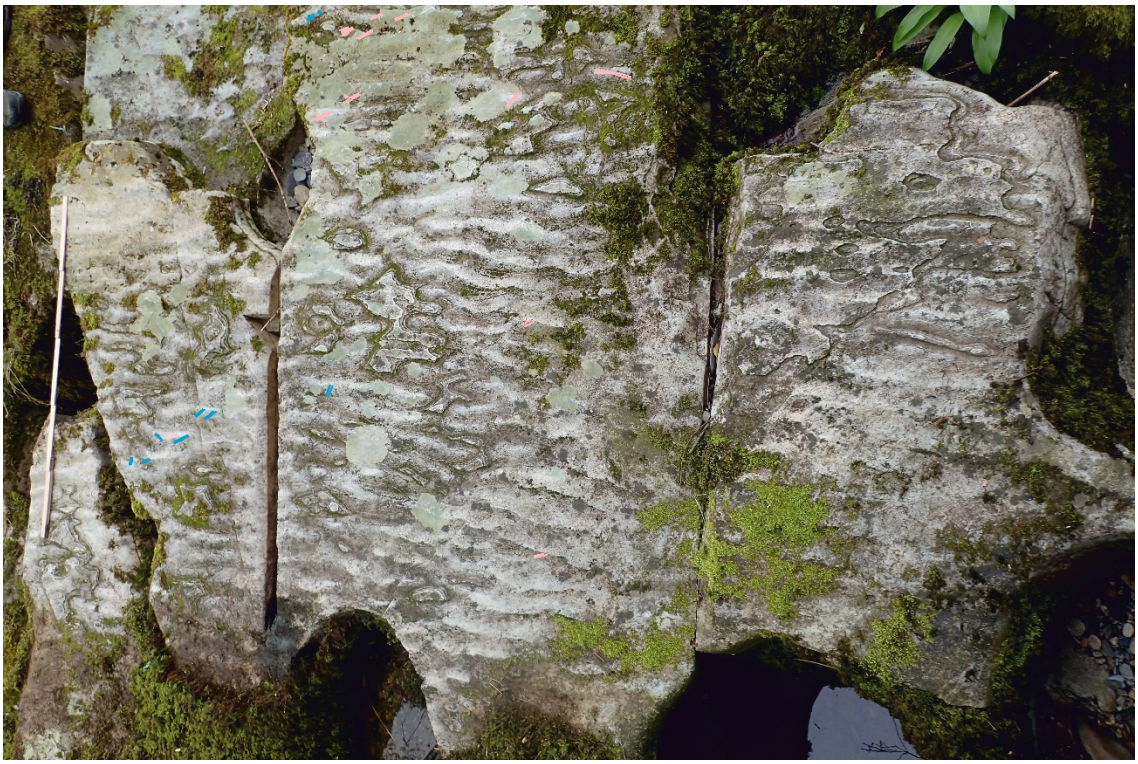

Figure S3. ***Surface B (ruler is 1 meter).***

Figure S4. ***Surface C1 (ruler is 1 meter).***

Figure S5. ***Surface C2 (ruler is 1 meter).***

Figure S6. ***Surface D (ruler is 1 meter).***

Surface	Location	Local Strat (Fig 1C)	Regional Strat.	Latitude	Longitude	Lithology	Surface area	Primary Surface Features	Number of Traces		
									Diplichnites	*Diplopod.*	Transitional
A	Lum Pot, North Side of River Lickle	15.50 m	Wallowbarrow	54° 18' 12.16" N	3° 12' 16.65" W	Tuff	0.14 m^2	Brittle failure scarps? (may be secondary)	0	2	0
B	Lum Pot, North Side of River Lickle	22.56 m	Wallowbarrow	54° 18' 12.79" N	3° 12' 15.39" W	Tuff	2.86 m^2	Wave Ripples	8	10	1
C1	Lum Pot, North Side of River Lickle	22.61 m	Wallowbarrow	54° 18' 12.85" N	3° 12' 15.56" W	Tuff	1.96 m^2	Brittle failure scarps? (may be secondary)	4	24	3
C2	Lum Pot, South Side of River Lickle	22.61 m	Wallowbarrow	54° 18' 12.41" N	3° 12' 15.16" W	Tuff	1.11 m^2	Low amplitude ripples, Pumice, Bedding sags	3	4	1
D	Lum Pot, North Side of River Lickle	22.92 m	Wallowbarrow	54° 18' 13.45" N	3° 12' 14.41" W	Tuff	1.92 m^2	Erosional furrows, Brittle failure scarps	25	66	7
X	Sour Milk Gill, Seathwaite	Unknown	Unknown	54° 29' 57.30" N	3° 11' 36.66" W	Sandstone?	0.01 m^2	None	3	0	0

Table S1. Contextual information for trackway surfaces studied in this paper (A-D) and Johnson et al. (1994) (C1, X).

THIN SECTION IMAGES

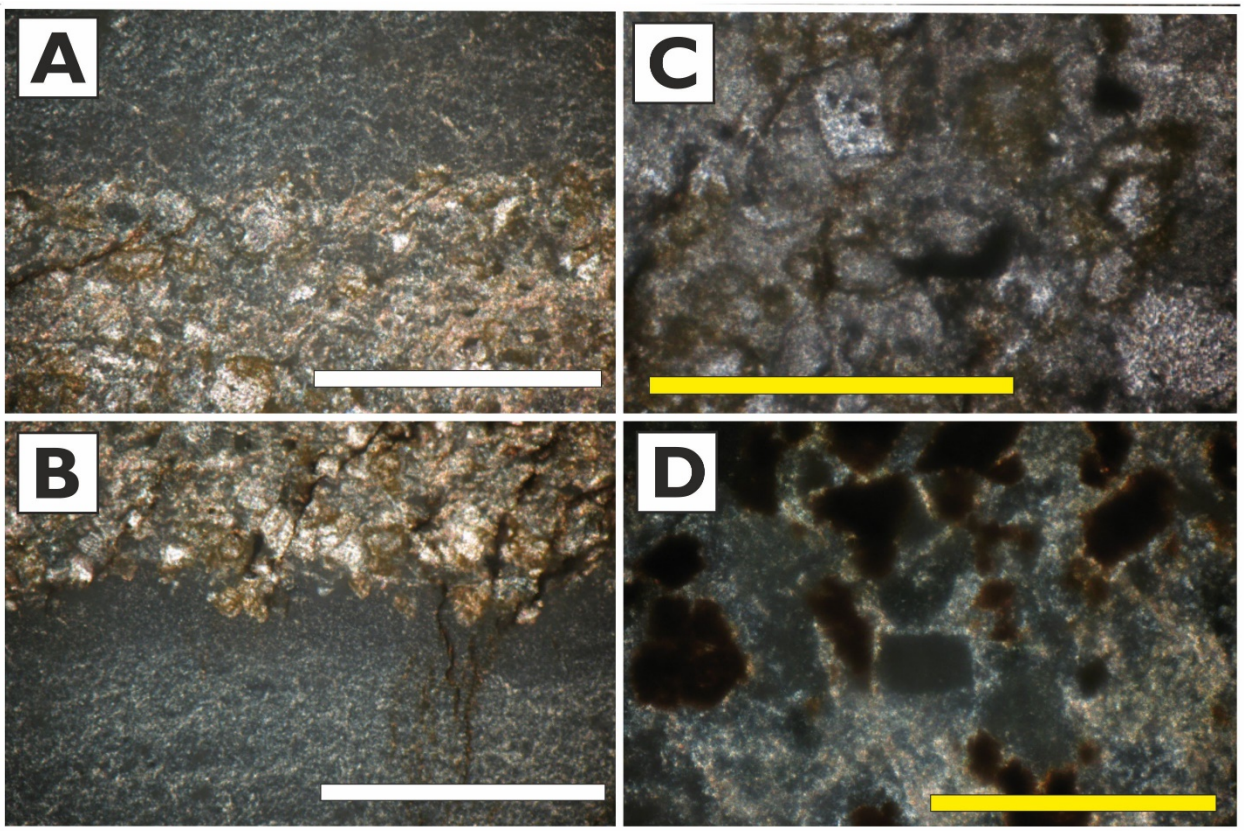

Figure S7. Images of tuff in thin section: A) Bottom of 3 mm-thick coarser ash fall layer (see Figure 2G), showing feldspar-dominated grains settling into cryptocrystalline ash [Surface C2]; B) top of same layer, succeeded by more fine ash [Surface C2]; C) subhedral alkali feldspar grains [Surface C2]; D) subhedral opaque oxides [8.1 m]. Scale bars 0.5 mm (white), 0.25 mm (yellow).

SUBSTRATE FIRMNESS

The Lum Pot succession contains evidence that the substrates traversed by the tracemakers had varying degrees of consolidation, irrespective of how wet they were (Table S2). The different material properties of these substrates placed a control on the potential for trackways to be emplaced. The table below shows the suspected likelihood of trackways on substrates of different firmness in different states of moistness, and instances where these were seen.

			Potential Trackways		Seen Trackways	
Substrate firmness	Examples (Figures)	Evidence	Wet	Dry	Wet	Dry
Unconsolidated (granular)	2F, 2H, 2I, 2J, 2K, 3B	Various soft-sediment deformation structures, ripple marks	N	Y	N	Y
Semi-firm (cohesive)	2A, 3D, 3F, 3H	Furrowed erosion surface indicating erosion down to a more cohesive layer within ash deposit	Y	?	Y	?
Firm (cohesive)	2N, 3G	Brittle syn-sedimentary deformation, fracture scarps	Y	N	Y	N

Table S2. Evidence for unconsolidated, semi-firm and firm ash substrates in the Lum Pot section and their propensity for being imparted with trackways when wet and dry.

TRACKWAY MORPHOLOGY

The plots shown in Figure 3I-K show the morphometric characteristics of the trackways (measurements in Tables S3-S5 at the end of this appendix). All trace fossil dimensions were corrected to account for a regional tectonic shortening of approximately 30%, with the direction of shortening determined from the cleavage in each trackway-hosting bed (Johnson et al., 1994). Figure 3J (shown in full as Figure S8, and including the three trackways from Sour Milk Gill)

shows how the width of the trackways is consistent regardless of length or ichnogenera, supporting the notion of a single type of tracemaker.

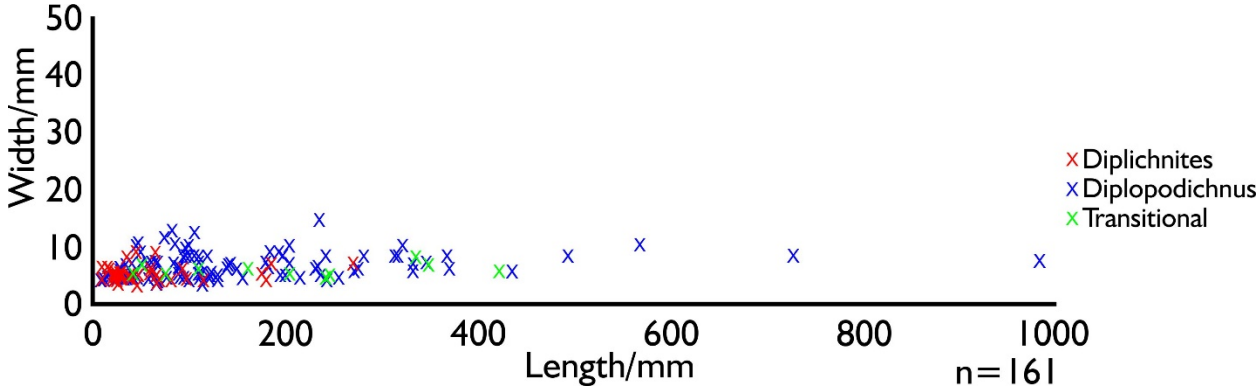

Figure S8. ***Length-width graph shows that all traces are of similar width, fitting very closely to a normal distribution (standard deviation = 2.04). The lengths of the traces have a much greater range and far higher standard deviation (=135.93) highlighting the more variable nature of the values.***

The graph showing sinuosity against length (Figure 3I, S9) shows that *Diplopodichnus* tracks, reflecting slow moving and wobbling tracemakers, were more likely to be long and looping than the *Diplichnites* tracks. Looping, common in mortichnial trails, was approximated with a measurement of sinuosity: the ratio of the length of a trace to its distance, where "distance" records the minimum distance between the end points of a trace in a straight line, and "length" records the distance between the end points of a trace when following the path of the trace.

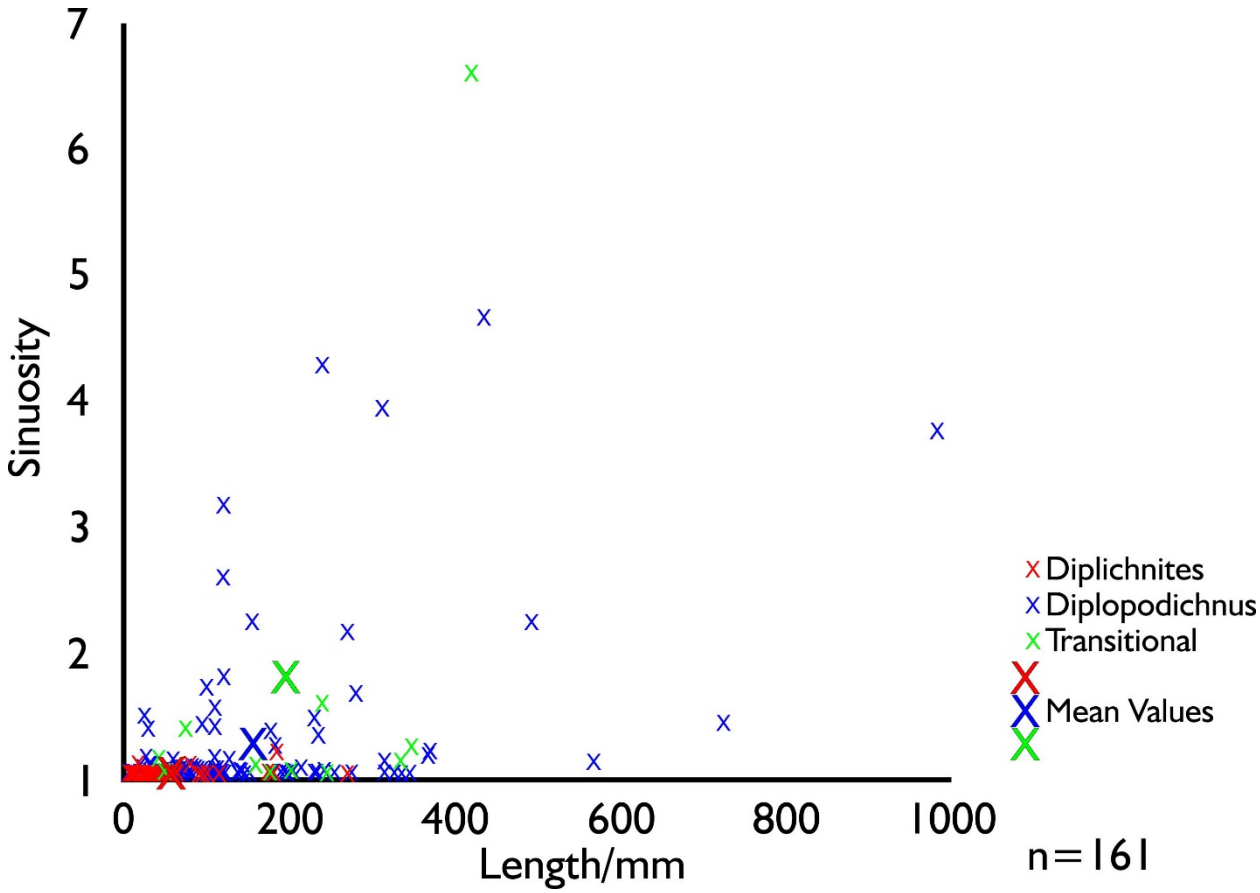

Figure S9. ***Sinuosity-length graph shows that most of the observed traces have a sinuosity below 1.1, including all but 3 examples of Diplichnites. Diplopodichnus and transitional forms exhibit a much greater range of sinuosities, and higher mean values.***

Looping of the trackways was further quantified as a ratio of the diameter of the loop in the region of the tightest curvature to the mean width of the trace along its length (Figure 3K; Figure S10). The degree of shortening in the Lickle area is reported to be approximately 30% (Johnson et al., 1994). This was corrected for using photo manipulation to artificially adjust the traces to their original proportions. Diameter was divided by trace width to produce a ratio comparable with other global examples of known or suspected mortichnia independent of the size of the trace maker. This was then presented as a histogram with bin size 4, starting from the minimum possible ratio (1.0). Published examples of arthropod mortichnia that were measured for comparison included the death trail of a Jurassic xiphosauran (in Barthel et al., 1990; their Fig.

5.5; ‘e’ in Figure 3K) and Cambrian euthycarcinid (in Collette et al., 2010; their Fig. 3D; ‘b’ in Figure 3K). Unpublished instances are shown in Figures S11-15. Myriapod death trails illustrated by Martins-Neto and Gallego (2006) are omitted as no scale was shown with their image (their Fig. 4D).

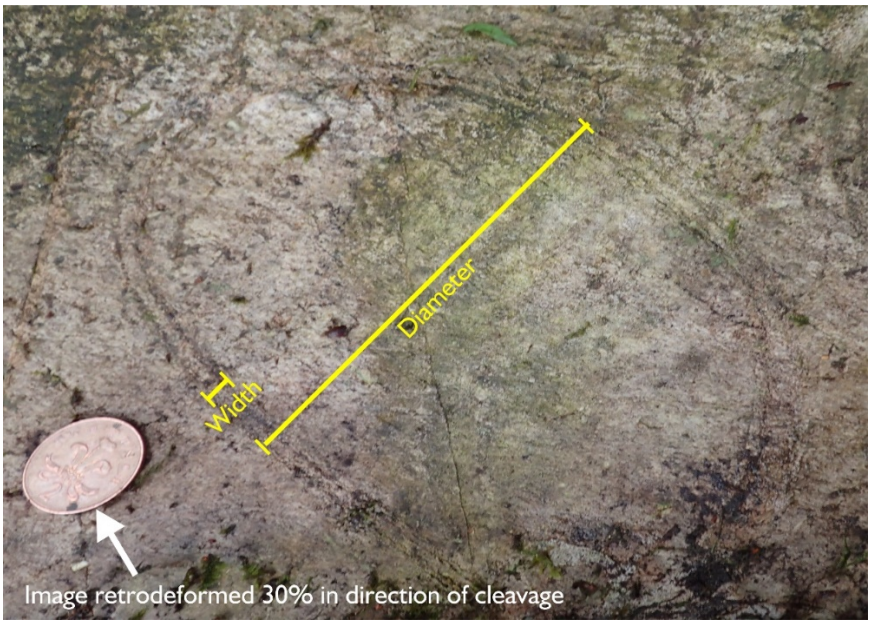

Figure S10. ***Measurements taken in the construction of Figure 3K (example is on Surface C1).***

Figure S11. ***Self-crossing looping trail of a dying dipteran trapped on the surface of a pond. Murchison River, Western Australia ('c' in Fig. 3K).***

Figure S12. ***Looping and self-crossing mortichnia of a dead silverfish (Zygentoma) observed on modern mudflat. Hastings, Sussex, UK ('d' in Fig. 3K).***

Figure S13. ***Detail of Figure S12 showing irregular widening of trail as dying silverfish wobbling and walked in circles.***

Figure S14. ***Detail of Figure S12 showing irregular widening of trail as dying silverfish wobbling and walked in circles.***

Figure S15. ***Suspected but unconfirmed mortichnial trail of a myriapod in the Silurian Tumblagooda Sandstone, Western Australia. Facies Asssociation 2 of this formation contains hundreds of examples of Diplichnites but this is the only trail to show looping, suggesting a***

rarer form of behavior (i.e., suspected to be dying) than other trackways in the formation ('a' in Fig. 3K).

OTHER COMPARATIVE NEOICHNOLOGY

Comparative neoichnology also provides analogues for instance where footprints are seen only on ripple crests (i.e., where dry granular sediment on ripple crestlines preserves footprint indents, but saturated granular sediment within troughs cannot retain such impressions). Figures S16-17 show examples of similar arthropod traces within damp fine-grained sands within an intertidal zone (Rainy Cove, Nova Scotia, Canada).

Figure S16. ***Preservation of footprint indents on damp ripple crests, but absent in waterlogged ripple troughs. Intertidal sands at low tide, Rainy Cove, Bay of Fundy, Nova Scotia, Canada.***

Figure S17. ***Preservation of footprint indents on damp ripple crests, but absent in waterlogged ripple troughs. Intertidal sands at low tide, Rainy Cove, Bay of Fundy, Nova Scotia, Canada.***

COMPARISON WITH OTHER PALAEOZOIC ICHNOFAUNAS

Classical multivariate cluster analysis was performed using Ward's method with a Euclidean similarity index in order to compare the ichnofaunal assemblage of the Wallowbarrow Tuff Formation with other Palaeozoic ichnofaunas. Analysis was performed using PAST (PAlaeontological STatistics) software (https://folk.uio.no/ohammer/past/). The known trace fossil assemblages from all formations grouped as Cambrian-Ordovician Coastal, Silurian Coastal, Silurian Alluvial and Lacustrine, Devonian Coastal and Devonian Alluvial and Lacustrine were used for comparison (utilizing ichnofaunal lists in Minter et al., 2016: see Table S6). While the Silurian and Devonian ichnofaunas grouped together in one cluster, the

Wallowbarrow assemblage is more similar in composition to the limited arthropod trackway ichnofaunas of other Cambrian and Ordovician littoral successions.

DATA TABLES

Table S3. Measurements of individual traces on each trackway surface (see Table S1) (trace fossil type shown as A = Diplichnites, B = Diplopodichnus, AB = Transitional forms).

Surface	Trace #	Distance	Length	Width	Sinuosity	A/B?
X	1	92	93	6	1.01	A
X	2	64	67	5	1.05	A
X	3	48	48	5	1.00	A
A	1	200	205	10	1.03	B
A	2	315	323	10	1.02	B
B	1	173	237	5	1.37	B
B	2	240	247	5	1.03	AB
B	3	113	113	3	1.00	B
B	4	63	67	3	1.05	B
B	5	25	25	4	1.00	A
B	6	20	20	4	1.00	A
B	7	270	270	7	1.00	A
B	8	30	30	5	1.00	A
B	9	45	45	9	1.00	A
B	10	100	100	4	1.00	B
B	11	50	50	9	1.00	B
B	12	200	200	5	1.00	B
B	13	40	40	5	1.00	B
B	14	35	35	8	1.00	A
B	15	40	40	5	1.00	A
B	16	30	30	5	1.00	A
B	17	130	130	4	1.00	B
B	18	195	195	5	1.00	B
B	19	300	370	6	1.23	B
C1	1	44	47	4	1.05	B
C1	2	18	27	4	1.50	B
C1	3	71	111	4	1.56	B
C1	4	27	27	4	1.00	B
C1	5	91	91	4	1.00	B
C1	6	40	42	4	1.06	B
C1	7	38	120	4	3.18	B

C1	8	18	18	4	1.00	B
C1	9	22	24	4	1.10	B
C1	10	62	64	6	1.04	B
C1	11	69	156	4	2.26	B
C1	12	24	29	4	1.18	B
C1	13	67	96	4	1.43	B
C1	14	64	64	4	1.00	B
C1	15	22	31	4	1.40	B
C1	16	44	44	4	1.00	B
C1	17	151	242	4	1.60	AB
C1	18	29	29	4	1.00	A
C1	19	196	216	4	1.10	B
C1	20	27	27	4	1.00	B
C1	21	38	120	4	3.18	AB
C1	22	93	436	6	4.67	B
C1	23	47	122	4	2.62	B
C1	24	33	33	4	1.00	B
C1	25	25	25	4	1.00	A
C1	26	153	186	7	1.22	A
C1	27	322	333	7	1.03	B
C1	28	64	422	6	6.61	AB
C1	29	125	272	6	2.18	B
C1	30	328	333	6	1.02	B
C1	31	39	39	4	1.00	A
C2	1	60	60	6	1.00	A
C2	2	150	150	6	1.00	B
C2	3	110	110	6	1.00	AB
C2	4	110	110	8	1.00	B
C2	5	115	115	4	1.00	A
C2	6	50	50	7	1.00	B
C2	7	65	65	9	1.00	A
C2	8	95	95	8	1.00	B
D	1	306	367	8	1.20	B
D	2	300	316	8	1.05	B
D	3	82	90	6	1.10	B
D	4	167	282	8	1.68	B
D	5	102	106	8	1.04	B
D	6	65	67	7	1.03	B
D	7	190	198	8	1.04	B
D	8	104	106	8	1.02	B
D	9	144	184	9	1.28	B

D	10	249	256	4	1.03	B
D	11	20	20	4	1.00	A
D	12	278	349	7	1.26	AB
D	13	58	58	7	1.00	B
D	14	49	51	7	1.05	AB
D	15	266	276	6	1.04	B
D	16	230	244	4	1.06	B
D	17	184	194	9	1.05	B
D	18	56	60	6	1.07	B
D	19	60	60	6	1.00	A
D	20	156	232	6	1.49	B
D	21	136	140	6	1.03	B
D	22	294	336	8	1.14	AB
D	23	196	204	7	1.04	B
D	24	85	91	6	1.08	B
D	25	121	123	5	1.02	B
D	26	96	96	10	1.00	B
D	27	230	234	6	1.02	B
D	28	96	98	4	1.02	A
D	29	30	30	5	1.00	A
D	30	13	13	4	1.00	B
D	31	31	31	5	1.00	A
D	32	62	68	4	1.09	B
D	33	64	67	4	1.05	A
D	34	41	43	4	1.07	B
D	35	90	90	5	1.00	B
D	36	31	34	7	1.11	B
D	37	498	568	10	1.14	B
D	38	59	59	6	1.00	B
D	39	54	76	5	1.41	AB
D	40	34	34	4	1.00	B
D	41	132	141	7	1.06	B
D	42	25	25	3	1.00	A
D	43	219	494	8	2.26	B
D	44	502	727	8	1.45	B
D	45	100	100	8	1.00	B
D	46	96	96	8	1.00	B
D	47	56	242	8	4.30	B
D	48	52	60	7	1.16	B
D	49	46	48	10	1.05	B
D	50	58	58	4	1.00	B

D	51	75	75	11	1.00	B
D	52	21	21	4	1.00	B
D	53	345	347	7	1.01	B
D	54	145	161	6	1.11	AB
D	55	78	110	7	1.42	B
D	56	106	106	12	1.00	B
D	57	8	8	4	1.00	B
D	58	104	113	5	1.08	B
D	59	29	29	6	1.00	B
D	60	233	235	15	1.01	B
D	61	177	183	6	1.04	B
D	62	21	21	5	1.00	A
D	63	112	129	5	1.16	B
D	64	82	84	7	1.02	B
D	65	75	82	13	1.11	B
D	66	39	41	7	1.05	B
D	67	84	86	10	1.02	B
D	68	94	110	5	1.17	B
D	69	278	316	8	1.14	B
D	70	16	18	6	1.13	A
D	71	20	20	4	1.00	A
D	72	192	204	5	1.06	AB
D	73	16	16	5	1.00	A
D	74	22	22	4	1.00	A
D	75	37	43	5	1.17	AB
D	76	10	10	4	1.00	A
D	77	63	65	7	1.03	B
D	78	129	180	7	1.40	B
D	79	80	314	8	3.95	B
D	80	73	82	4	1.11	A
D	81	59	59	5	1.00	A
D	82	69	69	4	1.00	A
D	83	176	180	4	1.02	A
D	84	167	176	5	1.05	A
D	85	15	15	6	1.00	A
D	86	46	46	3	1.00	A
D	87	10	10	6	1.00	A
D	88	17	17	5	1.00	A
D	89	25	25	5	1.00	A
D	90	58	100	10	1.74	B
D	91	45	45	10	1.00	B

D	92	48	48	5	1.00	A
D	93	119	119	8	1.00	B
D	94	260	983	7	3.78	B
D	95	67	121	5	1.81	B
D	96	25	25	4	1.00	A
D	97	70	77	4	1.10	B
D	98	144	144	7	1.00	B

Table S4. Measurements of looping in fully self-crossing Diplopidichnus trackways.

Surface	Loop diameter	Track width	D/W
C1	33	6	5.6
C1	44	6	7.4
C1	33	6	5.6
C1	16	6	2.6
C1	24	4	6.1
C1	29	4	7.2
C1	103	6	17.1
C1	128	6	21.3
D	69	8	8.6
D	96	8	12.0
D	65	8	8.2
D	102	8	12.8
D	71	7	10.1
D	56	7	8.0
D	92	7	13.1

Table S5. Average trackway dimensions.

		Av. Sinuosity	Av. Length	Av. Width	Number
Diplichnites	A	1.02	56	5	43
Diplopodichnus	B	1.28	153	7	106
Transitional	AB	1.80	197	6	12

Table S6. Data matrix compiled from Minter et al. (2016) and used for multivariate cluster analysis. 0 indicates absence and 1 indicates presence of a particular trace from the facies/age combination shown.

	C-O. Coastal	BVG	S. Coastal	S. Alluvial	D. Coastal	D. Alluvial
Diplichnites	1	1	1	1	1	1
Protichnites	1	0	1	0	0	1
Diplopodichnus	1	1	0	1	1	1
Palmichnium	1	0	1	1	1	1
Skolithos	0	0	1	1	1	1
Diplocraterion	0	0	1	0	1	1
Psammichnites	0	0	1	0	0	0
Daedalus	0	0	1	0	0	0
Palaeophycus	0	0	1	1	0	1
Arenicolites	1	0	1	1	1	1
Polarichnus	0	0	1	1	0	0
Arthraria	0	0	1	0	0	0
Bergaueria	0	0	1	0	0	0
Cochlichnus	0	0	1	1	0	1
Gordia	0	0	1	0	0	0
Cruziana	0	0	1	1	1	1
Monomorphichnus	0	0	1	1	1	0
Helicodromites	0	0	1	0	0	0
Chondrites	0	0	1	0	1	0
Protovirgularia	0	0	1	0	1	0
Petalichnus	0	0	1	0	1	0
Beaconites	0	0	1	1	1	1
Syncoprulus	0	0	1	0	0	0
Didymaulichnus	0	0	1	1	1	0
Rhizocorallium	0	0	1	0	0	0
Heimdallia	0	0	1	0	1	0
Didymauliponomos	0	0	1	0	1	0
Helminthopsis	0	0	1	0	1	0
Crescentichnus	0	0	1	0	1	1
Taenidium	0	0	1	0	1	1
Rusophycus	0	0	1	1	1	1
Tumblagoodichnus	0	0	1	0	0	1
Planolites	0	0	1	1	1	1
Paleohelcura	0	0	1	1	0	1
Siskemia	0	0	1	0	0	1

Merostomichnites	0	0	1	1	0	1
Oniscoidichnus	0	0	1	0	0	0
Stiaria	0	0	1	0	0	1
Steinsfjordichnus	0	0	1	0	0	0
Scoyenia	0	0	1	0	0	1
Striatichnium	0	0	1	0	0	0
Spirophyton	0	0	0	0	1	0
Teichichnus	0	0	0	0	1	0
Lockeia	0	0	0	0	1	0
Maculichna	0	0	0	0	1	0
Asterosoma	0	0	0	0	1	0
Lanicoidichna	0	0	0	0	1	0
Agrichnium	0	0	0	0	1	0
Treptichnus	0	0	0	0	1	1
Lophoctenium	0	0	0	0	1	0
Halopoa	0	0	0	0	1	1
Svalbardichnus	0	0	0	0	0	1
Striatichnium	0	0	0	0	0	1
Stiallia	0	0	0	0	0	1
Undichna	0	0	0	0	0	1
Danstairia	0	0	0	0	0	1
Keircallia	0	0	0	0	0	1
Mitchellichnus	0	0	0	0	0	1
Scolicia	0	0	0	0	0	1
Mermia	0	0	0	0	0	1
Asterichnus	0	0	0	0	0	1
Bifungites	0	0	0	0	1	0
Cylindricum	0	0	0	0	1	0
Thalassinoides	0	0	0	0	1	0
Gyrichnites	0	0	0	0	0	1
Pustulichnus	0	0	0	0	0	1
Entradichnus	0	0	0	0	0	1
Ancorichnus	0	0	0	0	0	1
Cornulatichnus	0	0	0	0	0	1
Kouphichnium	0	0	0	0	1	0
Nereites	0	0	0	0	1	0
Total	5	2	40	16	35	38

LARGER IMAGES OF PHOTOGRAPHS SHOWN IN FIGURES 2 AND 3

Figure 2. Sedimentological characteristics of the trackway-bearing tuffs at Lum Pot [position on Figure 1C log or trackway surface in square brackets]. A) Furrowed grooves developed as overlying ash eroded down to a new semi-firm substrate, later traversed by Diplichnites and Diplopodichnus [Surface D]; B) Unconsolidated substrate revealed by reworking of tuff into bifurcating wave ripple marks. Surface hosts multiple short (<15 cm) trackways (not visible at this scale; locations starred) [Surface B]; C) Homogenous tuff with two vesicular horizons [20.7 m]; D) Pumice clasts (pink arrow) with similar-sized weathered out holes (yellow arrow), plan-view of exposed internal part of tuff bed [22.4 m]; E) Coarse layer of settled ash [1 cm below Surface C2]; F) Aggradational climbing wave ripples in cross section, indicating continuous ash deposition in agitated water [14.0 m]; G) Consolidated substrates revealed by vertical section through small brittle faults and fractures. Overlying 30 cm tuff bed has a horizontal upper bounding surface [21.1 m]; H) Bedding sags arising from impacting ejecta onto a wet substrate. Arrow points to Diplichnites (not visible at this scale) which descends over lip of crater and into sag [Surface C2]; I) Soft-sediment deformation arising from liquefaction of saturated, unconsolidated ash [13.6 m]; J) Banded tuff (B) passing vertically into large ball-and-pillow structures (BP) indicating instance of wholly unconsolidated and liquefied sediment [21.8 m]. Scale bars: 10 cm (black); 1 cm (red). See Appendix for larger photographs.

A

B

C

D

E

F

G

H

I

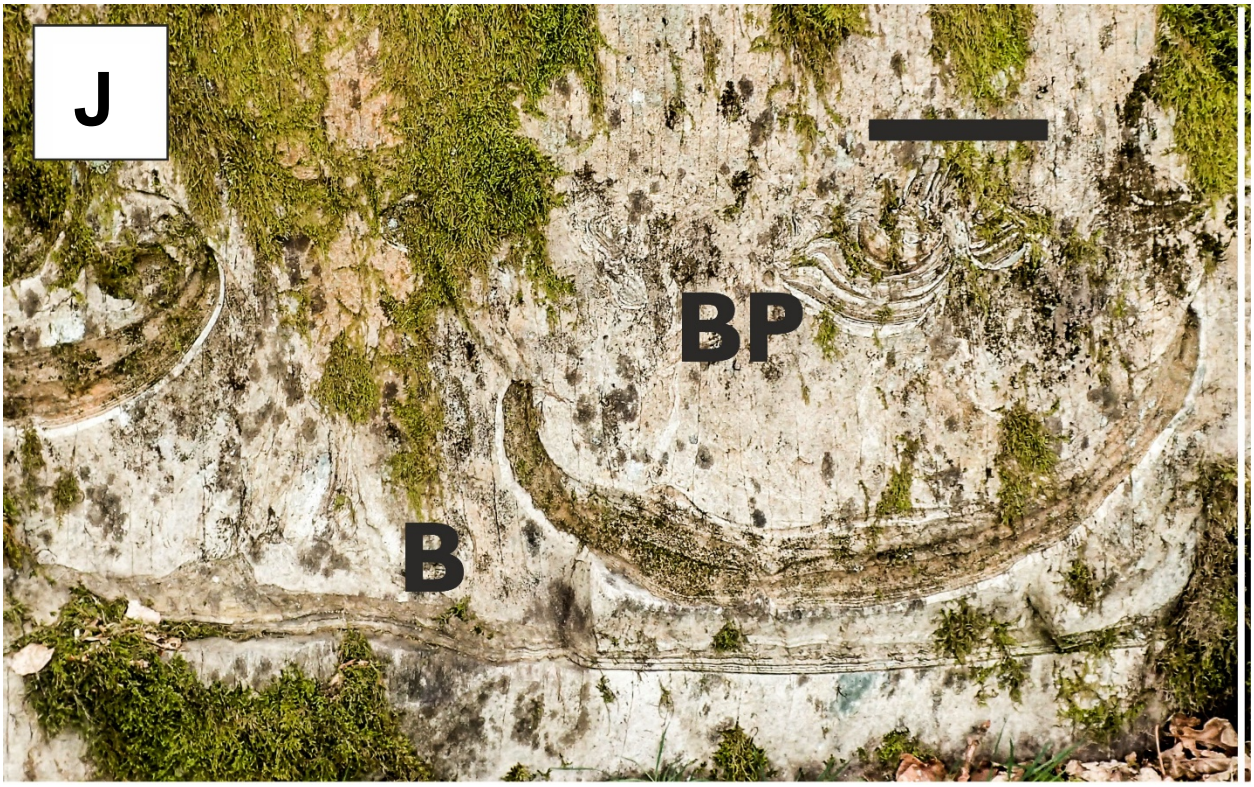
J
BP
B

Figure 3. Distribution and form of trackways. B) *Diplichnites* restricted to ripple crests on Surface B, sketch shows measured transect of surface topography and distribution of trackways in pink; D) *Diplopodichnus* following microtopography of furrowed Surface D, with sketch as in Figure 3C; F) Evidence for probing behaviour at a curve in a *Diplichnites* trackway [Surface D]; G) Planview of a microfault scarp (top and bottom highlighted in blue) showing *Diplichnites* passing over scarp lip from left, and rejoining lower foot of scarp at a distance as tracemaker stepped downwards [Surface D]; H) Transition from *Diplichnites* to *Diplopodichnus* along same trackway [Surface D].

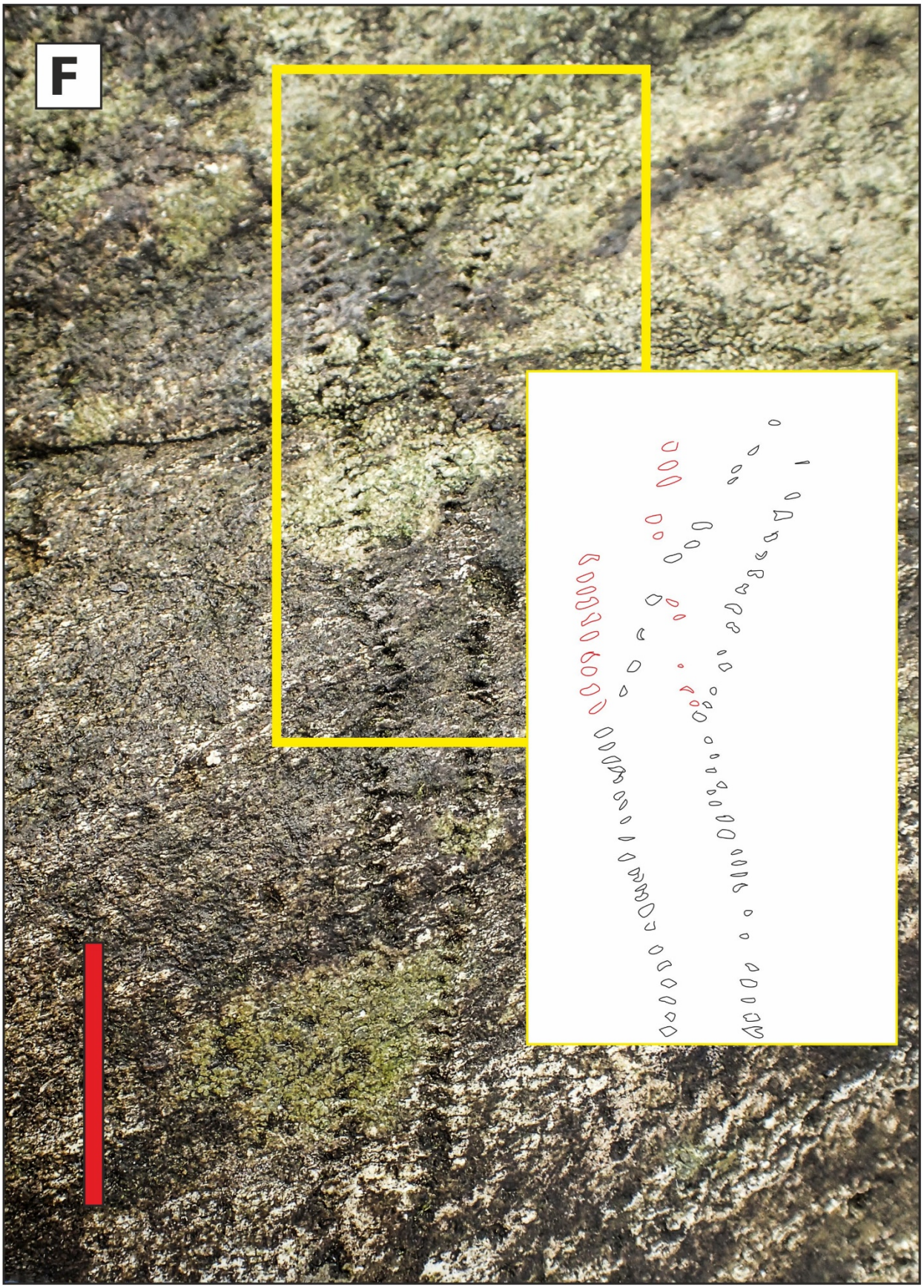
F

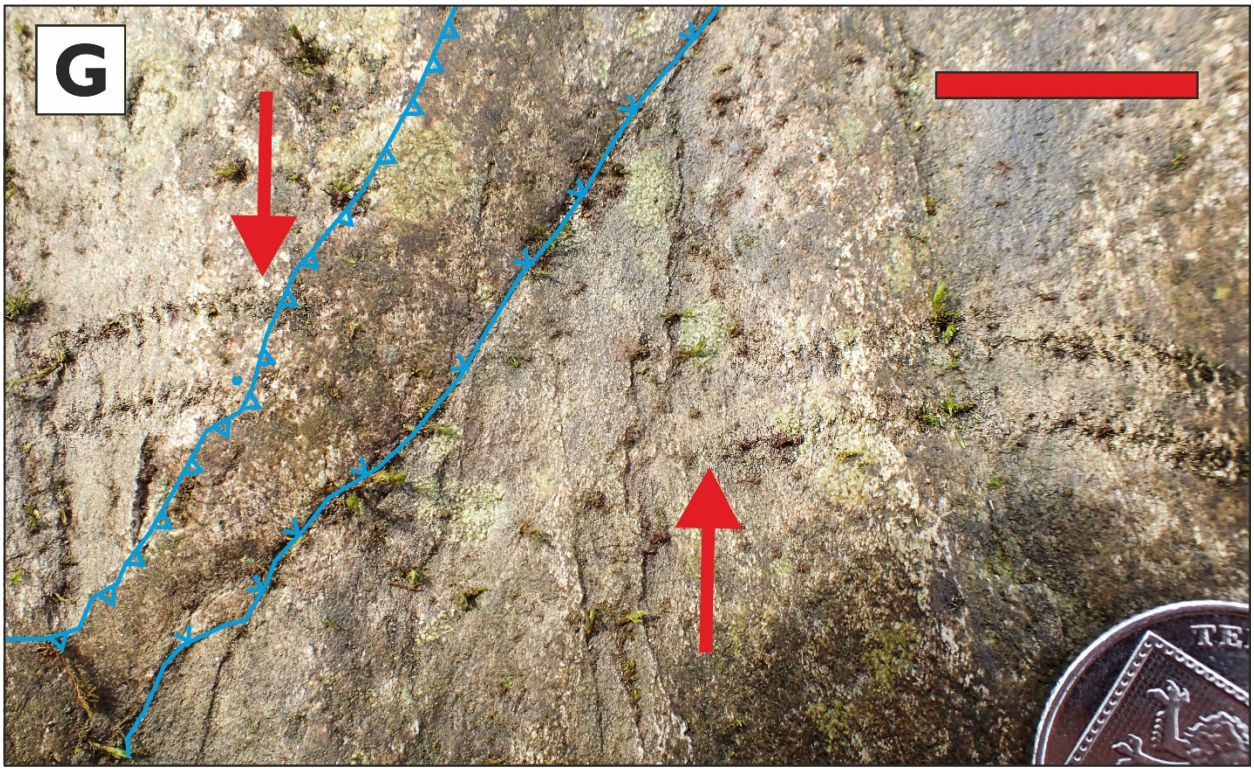
G

H
Diplapodichnus
Diplichnites